Zebrafish (Danio rerio) Oatp2b1 as a Functional Ortholog of the Human OATP2B1 Transporter

Jelena Dragojević
Ruder Boskovic Institute: Institut Ruder Boskovic
Nikola Maraković
Institute for Medical Research and Occupational Health: Institut za medicinska istrazivanja i medicinu rada
Marta Popović
Ruder Boskovic Institute: Institut Ruder Boskovic
Tvrtko Smital (smital@irb.hr)
Ruder Boskovic Institute: Institut Ruder Boskovic https://orcid.org/0000-0003-2890-3394

Research Article

Keywords: OATP2b1/Oatp2b1, zebrafish, transient and stable transfectants, homology model, substrate preferences, functional orthology

Posted Date: April 8th, 2021

DOI: https://doi.org/10.21203/rs.3.rs-385965/v1

Version of Record: A version of this preprint was published at Fish Physiology and Biochemistry on September 21st, 2021. See the published version at https://doi.org/10.1007/s10695-021-01015-7.

Abstract

OATP2B1 belongs to a highly conserved organic anion transporting polypeptide (OATP) family of transporters, involved in the cellular uptake of both endogenous and exogenous compounds. The main substrates of human OATP2B1 include steroid conjugates, bile salts and thyroid hormones, as well as several pharmaceuticals. Human *OATP2B1* has orthologous genes in other vertebrate species, including zebrafish (*Danio rerio*), a widely used model organism in biomedical and environmental research. Our previous studies showed that zebrafish Oatp2b1 was phylogenetically closest to mammalian OATP2B1/Oatp2b1 and that it shares a similar tissue expression pattern. In this study, we aimed at discovering whether zebrafish Oatp2b1 could be a functional ortholog of human and rodent OATP2B1/Oatp2b1. To test this hypothesis, our primary goal was to obtain the first *in vitro* and *in silico* insights related to the structure and potential substrate preferences of zebrafish Oatp2b1. We generated cells transiently and stably transfected with zebrafish Oatp2b1 cloned from zebrafish liver, constructed an Oatp2b1 homology model, developed transport activity assays with model fluorescent substrate Lucifer yellow, and finally utilized this assay to analyze the interaction of zebrafish Oatp2b1 with both physiological and xenobiotic substances. Apart from structure similarities, our data revealed the strongest interaction of zebrafish Oatp2b1 with bile acids, steroid sulfates, thyroid hormones and bilirubin, as well as xenobiotics bromosulfophthalein and sulfasalazine, which indicates its functional orthology with human OATP2B1.

1. Introduction

Members of the organic anion transporting polypeptide superfamily (OATP in humans/Oatp in other animals) are transmembrane proteins involved in the trafficking of large amphipatic molecules across the plasma membrane of eukaryotes. OATPs/Oatps mediate the transport of a wide range of endogenous (steroid hormones, bile salts, prostaglandins) and exogenous compounds (pharmaceuticals, natural toxins). Their role in ADME processes (absorption, distribution, metabolism and elimination) has become increasingly recognized due to their involvement in the cellular uptake of drugs in tissues important for pharmacokinetics, such as the liver, kidney and intestines (Kindla et al., 2009). Also, their high conservation across many species has been attributed to their central role in detoxification processes (Meier-Abt et al., 2006).

OATPs/Oatps have been classified into six subfamilies (OATP1-6) with OATP1/Oatp1 being the most extensively studied for their link to human diseases and cancer treatment (Hagenbuch and Meier, 2004; Hagenbuch and Stieger, 2013). The OATP2/Oatp2 subfamily includes two transporters, OATP2A1/2a1 and OATP2B1/2b1 in humans, mice and rats. OATP2B1, originally isolated from the human brain (Hagenbuch & Meier, 2003; Kullak-Ublick et al., 2001; Tamai et al., 2000), is one of the most important members of the OATP family, along with OATP1B1 and OATP1B3. It is a 709-amino acid glycoprotein containing 12 putative transmembrane-spanning domains (TMDs) (Hagenbuch and Meier, 2004). Unlike other members of this sub-family, OATP2B1/Oatp2b1 is ubiquitously expressed across tissues in humans

and rats. It is the third most expressed OATP in the basolateral hepatocyte membrane of the human liver (Kullak-Ublick et al., 2001; Tamai et al., 2000).

It has been shown that human OATP2B1 transports physiological substrates including steroid conjugates estrone 3-sulfate (E3S) and dehydroepiandrosterone sulfate (DHEAS), bile salt taurocholate and thyroid hormone thyroxine (T4), as well as several pharmaceuticals including statins, fexofenadine and glibenclamide (Hagenbuch and Gui, 2008; Roth et al., 2011). A significant overlap in substrate specificities of OATP2B1 and the hepatic OATPs (OATP1B1 and OATP1B3) has been observed (McFeely at al., 2019). The transport mechanism for OATP2B1 has still not been resolved, but based on homology models for OATP1B1 and OATP2B1 of distantly related major facilitator superfamily (MFS) members in bacteria, glycerol-3-phosphate transporter and lactose permease, it has been suggested that TMDs form a positively charged pore through which substrates are translocated in a rocker switch type of mechanism (Maier-Abt et al., 2005, Roth et al., 2012). It has been observed that OATP2B1 transport is enhanced by acidic pH, and proton gradient is considered to be the driving force (Nozawa et al. 2004; Sai et al. 2006).

In zebrafish, the Oatp superfamily consists of five families (Oatp1-5) that include 14 genes (Oatp1c1, Oatp1d1-2, Oatp1f1-4, Oatp2a1, Oatp2b1, Oatp3a1-2, Oatp4a1, Oatp5a1-2), out of which six members are found only in fish lineage (Oatp1d1, Oatp1e1 and Oatp1f1–4) (Meier-Abt et al., 2005; Popovic et al., 2010). Tissue-specific gene expression, as determined by qPCR, revealed the highest expression of zebrafish Oatp2b1 in the gills of both sexes, followed by high expression in the brains, kidneys and intestines of females, and high expression level in the intestines, kidneys, testes and brains of males. Moderate expression of Oatp2b1 was observed in zebrafish ovaries, and the liver of both sexes (Popovic, 2014).

However, despite its expression in toxicologically relevant tissues and putative role in cellular detoxification, as well as its possible physiological importance, Oatp2b1 has been poorly studied in non-mammalian species. Due to a high conservation of OATPs/Oatps across vertebrates and a similar expression pattern with mammalian orthologs, we hypothesize that zebrafish Oatp2b1 could have a similar function as human/mammalian OATP2B1/Oatp2b1. Therefore, the primary goal of this study was to obtain initial *in vitro* and *in silico* insights related to the structure, substrate preferences and role of Oatp2b1 in zebrafish as a valuable model vertebrate species. To address this goal, we generated cells transiently and stably transfected with Oatp2b1 cloned from zebrafish liver, constructed homology model of zebrafish Oatp2b1, developed transport activity assays with model fluorescent substrate, and finally utilized this assay to analyze the interaction of Oatp2b1 with both physiological and xenobiotic substances.

2. Materials And Methods

2.1. Chemicals

All of the tested compounds, model fluorescent substrates and interactors alike were of the highest analytical grade and purchased from Sigma-Aldrich (Taufkirchen, Germany) or Alfa Aesar (Kandel, Germany).

2.2. Cloning and heterologous expression

A full-length zebrafish Oatp2b1 sequence was obtained from zebrafish cDNA by polymerase chain reaction using high fidelity Phusion DNA polymerase (Thermo Scientific, MA, USA) and specifically designed primers with NotI and HindIII restriction sites on the forward, and BglII and XbaI restriction sites on the reverse primers. An amplified DNA fragment was cloned into a linearized pJET 2.0 vector (Invitrogen, Carlsbad, CA). The sequence was verified by DNA sequencing using automated capillary electrophoresis (ABI PRISM® 3100-Avant Genetic Analyzer) at the Ruđer Bošković Institute DNA Service (Zagreb, Croatia). Sequenced genes of each clone were compared to the reported gene sequences from the NCBI and ENSEMBL databases. The verified sequence was subcloned into the pcDNA3.1(+) and pcDNA3.1/His vectors (Invitrogen, Carlsbad, CA). Transient transfection of human embryonic kidney cells (HEK293T) was based on a procedure previously described by Popovic et al. (2013) using polyethyleneimine (PEI) as the transfection reagent. To evaluate transfection efficiency, separate cells were transfected with pcDNA3.1/His/LacZ plasmid (Invitrogen, Carlsbad, CA) and transfection efficiency was evaluated 24 h after transfection with the LacZ staining protocol (Sambrook et al., 1989).

Stable expression of Oatp2b1 in genetically engineered HEK293Flp-In cells was achieved using targeted integration of Oatp2b1 sequence cloned into integration vector pcDNA5. pcDNA5/Oatp2b1 construct was specifically targeted into the genome of Flp-In-293 cell line following the manufacturer's instructions. In order to reach 90% confluence, Flp-In-cells were seeded in 6-well plates 48 h prior to transfection at a cell density of $3*10^5$ cells/cm^2, with a final volume of 2.5 mL per well. The transfection mixture consisted of 0.375 µg recombinant plasmid pcDNA5/FRT with inserted gene, 3.375 µg pOG44 plasmid and 3.750 µg PEI reagent (1:1 ratio with pcDNA5/Frt + pOG44). pcDNA5-FRT/pOG44/PEI mixture (250 µL) was added to each well with 2.25 mL of DMEM medium without FBS and incubated for 4 h at 37°C and 5% CO_2. After four hours, the medium with transfection mixture was replaced with 2.5 mL DMEM-FBS per well. The transfected cells were left to grow in standard conditions for 48 h, scraped off, transferred to 25 cm^2 cell culture flask, and left to adhere overnight. The next morning, after the cells adhered to the flask bottom, 100 µg/mL of hygromycin B was added and the cells were kept in DMEM-FBS + hygromycin B for 20–25 days with DMEM-FBS change every 3–4 days. After that period, only transfected cells (i.e. hygromycin resistant) survived and started to grow. The cells were then tested for uptake of fluorescent substrates and later used for transport activity assays.

2.3. Western blotting and cell localization

Cells were collected from two wells of a 6-well microplate 24 h after transfection and lysed in NP-40 (Nonidet buffer) with a protease inhibitors cocktail AEBSF (Sigma-Aldrich, Taufkirchen, Germany) for 30 min on ice. After the lysis, cells were briefly sonicated (5 s at 5 µm) and centrifuged at 4000 x *g* for 20 min at 4°C. Protein concentration in total cell lysate (TCL) was measured using Bradford assay (Bradford,

1976). Western blot analysis was performed using Mini-PROTEAN 3 Cell electrophoresis chamber for polyacrylamide gel electrophoresis, together with Mini Trans-Blot Cell transfer system (Bio-Rad Laboratories, CA, USA) for wet transfer. Proteins (20 µg per lane) were separated by electrophoresis in gradient (3–12%) polyacrylamide gel with 0.1% sodium dodecyl sulfate added and then transferred to the polyvinylidene difluoride membrane (Millipore, MA, US) via wet transfer (1 h at 80 V, with 0.025% SDS). Blocking was performed in blocking solution containing 5% low fat milk, 50 mM Tris, 150 mM NaCl and 0.05% Tween 20 for 1 h. Membranes were washed and incubated for 1 h with anti-Xpress antibody (Invitrogen, ThermoFisher Scientific, MA, USA) diluted 2500 x. Goat anti-mouse IgG-HRP (diluted 5000 ×) was used as a secondary antibody with a one-hour incubation period (Santa Cruz Biotechnology, CA, USA). Histone H2B antibody (Santa Cruz Biotechnology, INC) was used as the loading control. The proteins were visualized by chemiluminescence (Abcam, Cambridge, UK). Protein size was estimated by protein markers (ThermoFisher Scientific, MA, USA).

2.4. Homology modelling – human vs. zebrafish OATP2b1/Oatp2b1

Build Homology Models protocol as implemented in Biovia Discovery Studio Client v18.1. (Dassault Systèmes, Vélizy-Villacoublay, France) was used to construct both human and *Danio rerio* OATP2b1/Oatp2b1 homology models based on the alignment of the model sequence and the template structure - crystal structure of the glycerol-3-phosphate transporter from *Escherichia coli* (PDB ID: 1pw4) (F. Meier-Abt et al., 2006, Huang et al., 2003). To generate homology models, the Build Homology Models protocol uses the MODELER (Sali and Blundell, 1993) automodel. The input sequence alignment between the model sequence of the corresponding Oatp2b1 and the sequence of glycerol-3-phosphate transporter, necessary for building the homology model, was obtained using Align Sequences protocol (for hsOATP2b1 – Sequence Identity: 10.3 %, Sequence Similarity: 30,8 %; for drOatp2b1 – Sequence Identity: 9.6 %, Sequence Similarity: 28,4 %). After alignment analysis, long insertions that could not be modeled correctly were excised in order to obtain a reliable model. All insertions (the N-terminal variable region, the large extracellular and intracellular loops/regions) that were deemed to be unreliable were excised/removed. A structure-based sequence alignment of corresponding Oatp2b1 and glycerol-3-phosphate transporter template with the unmodeled extracellular and intracellular portions illustrated (underlined) are shown in Figures S5 and S6 in the Supplementary Material.

The remaining parameters in the Parameters Explorer of the Build Homology Models protocol were set as follows. Cut Overhangs was set to True to cut the terminal residues of the input model sequence that were not aligned with the templates. Number of Models was set to 10 to specify the number of models to create from an initial structure with Optimization Level set to High to define the proportion of molecular dynamics with simulated annealing to perform. As to building refinement models on detected loop regions, i.e., the model sequence regions of at least five residues length which are not aligned with the template, Refine Loops was set to True. Build Homology Models protocol uses the DOPE (Discrete Optimized Protein Energy) (Shen and Sali, 2006) method to refine loops. Refine Loops Number of Models was set to 5 to define the number of models to be created by loop optimization, and Refine Loops

Optimization Level was set to Low to define the number of models to be created by loop optimization. Refine Loops with Use Discrete Optimized Protein Energy (DOPE) Method was set to High Resolution.

After running Build Homology Models protocol, the Best Model Structure Superimposed to Templates was selected from the generated output models for the final three-dimensional model structure of Oatp1d1. Finally, the selected model was manually adjusted and minimized using Smart Minimizer algorithm. The dielectric constant to be used to minimize the OATP2b1/Oatp2b1 models was set to 2 corresponding to the dielectric properties of saturated hydrocarbons as instructed when modelling a membrane system. Dock Ligands (CDOCKER) protocol using full potential CHARMm force field for atom typing for docking Lucifer yellow inside a binding site defined as a sphere large enough to surround a central pore of corresponding Oatp2b1 homology model. The final pose representing predicted binding conformation of Lucifer yellow inside corresponding Oatp2b1 structure was selected based on the highest frequency among all generated poses (Fig. 7).

2.4. Transport activity assays

FlpIn/Oatp2b1 cells were grown in 96 well plates (density $8*10^5$ cells/ml) for 24 hours until they reached confluency. DMEM/FBS was removed and cells were preincubated in 100 µL of the transport medium (145 mM NaCl, 3 mM KCl, 1 mM $CaCl_2$, 5 mM glucose, 5 mM HEPES and 0.5 mM $MgCl_2$) for 10 min at 37°C. To assess the transport and dose response rates of fluorescent substrate LY, 25 µL of five times concentrated fluorescent substrate was added to the preincubation medium and incubated for 2.5 min at 37°C. The concentration range applied was 1–500 µM. Incubation time was determined based on the initial time response experiments (Fig. S1 in Supplementary Material). After the incubation, the cells were washed two times with 125 µL of cold transport medium and lysed with 0.1% of sodium dodecyl sulphate (SDS) for 30 min. Lysed cells were transferred to the 96-well black plates and the fluorescence was measured with a microplate reader (Infinite M200, Tecan, Salzburg, Austria). The transport rates were determined by subtracting the measured fluorescence of transfected cells with the fluorescence of non-transfected control cells. Normalization of the obtained fluorescence response was done using calibration curves obtained for each substrate, taking into account protein content. Calibration curves for fluorescent dyes were generated in 0.1% SDS and in the cell matrix dissolved in 0.1% SDS. Total protein concentration was measured using Bradford assay (Bradford, 1976). Using the calibration curves and total protein content, the uptake of the fluorescent substrates was expressed as nM of substrates per mg of protein per minute. After determination of transport kinetics for fluorescent dye, LY was used in subsequent inhibition assays. Inhibition measurements were based on the co-exposure of transfected cells and mock control with the determined model substrate and potential interactor. After 10 minutes of incubation, cells were incubated for 40 s with the test compounds, followed by 2.5 min incubation with LY. The concentration of model substrate used was in the linear part of the previously determined concentration-response curve. The interaction screens were initially performed with one concentration of tested compounds (100 µM), and for the most potent interactors detailed dose response experiments were performed and the respective IC_{50} values determined.

Type of interaction for the strongest interactors identified in the initial interaction screening was determined by comparing the kinetic parameters of LY uptake in the presence and absence of interacting compounds, where their concentrations corresponded to their previously calculated IC_{50} values. A competitive inhibitor (i.e. substrate) will cause an increase in K_m, but leave V_{max} unaffected. The presence of a noncompetitive inhibitor will decrease V_{max} and will not affect K_m. A third type of interaction is uncompetitive inhibition, where both V_{max} and K_m are decreased.

3. Results

3.1. Protein identification and cell localization

Western blot analysis of total cell lysate of HEK293/Oatp2b1 overexpressing cells revealed two distinct signals, a monomeric form of approximately 80 kDa, and an oligomeric band at > 200 kDa, with possible post-translational modifications that can be seen as smears above the monomeric and oligomeric bands. Histone H2B (18 kDa) served as a loading control (Fig. 1).

Immunofluorescence showed localization of zebrafish Oatp2b1 within the cell membrane of transiently transfected HEK293T cells. This was visualized by co-localization of the green colored Oatp2b1 (FITC) and red colored Na/K ATPase (CY3), which is normally localized in the cell membrane. As the result of co-localization, signals of the two dyes were combined and subsequently produced an orange signal which confirmed the localization of zebrafish Oatp2b1 within the cell membrane (Fig. 2). This result indicates that zebrafish Oatp2b1 protein is correctly localized and can be functional in the used expression system.

3.2. Homology modeling – human vs. zebrafish Oatp2b1

The generated models of human OATP2b1 and zebrafish Oatp2b1 are shown in Figs. 3 and 4, respectively. As they start from the same template structure (glycerol-3-phosphate transporter from *E. coli*), a great resemblance between the global structure of the two models is to be expected. Indeed, molecular overlay revealed a high degree of similarity with an overlay similarity ratio of 0.629017. More closer inspection revealed that the shortest distance between the residues defining the diameter of the active site at the closed end of the substrate-translocation pathway in the middle of the membrane is predicted to be shorter in case of zebrafish Oatp2b1 (12.6 Å vs. 13.6 Å in case of human OATP2b1). This is in agreement with the negligibly larger solvent accessible surface inside the active site in case of human OATP2b1.

Furthermore, using molecular docking we generated model complexes of the structural model of human or *Danio rerio* OATP2b1/Oatp2b1 and known model substrate LY (Fig. 5) with a binding sphere (r = 24.1 or 24.7 Å, respectively) defined large enough to encompass the majority of the central pore. For both models, LY is predicted to be positioned in the center of the transmembrane channel, validating the quality of the generated models.

3.2. Functional characterization of zebrafish Oatp2b1

3.2.1. Model substrate

Initial tests of anionic fluorescent dyes that could be used as substrates for functional characterization of zebrafish Oatp2b1 revealed Lucifer yellow (LY) as a potential fluorescent substrate under physiological conditions (pH 7.4). Time and dose response assays confirmed that LY is indeed an Oatp2b1 substrate, and its transport followed classical Michaelis-Menten kinetics (Fig. 6). The determined kinetic parameters of the LY transport in transfected cells at ph 7.4 resulted in a V_{max} value of 21.4 nmol/mg protein/min and K_m of 620.3 μM (Fig. 6).

However, as mammalian OATP2B1 shows an increase in transport activity at acidic pH, we performed an uptake transport assay with LY in acidic conditions (pH 5) as well, which indeed resulted in an increased transport rate of LY (V_{max} = 51.5 nmol/mg protein/min, K_m = 175.8 μM; Fig. 7).

Figure 6. Dose-response of zebrafish Oatp2b1 transport of the fluorescent model substrate LY (K_m = 620.3 μM) expressed as transport rate (nmol/mg protein/min) over LY concentration (μM) after 2.5 min incubation with LY at pH 7.4. Each data point represents the mean ± SE from triplicate determinations. Dotted lines represent confidence intervals.

Figure 7. Dose-response of zebrafish Oatp2b1 transport of the fluorescent model substrate LY (K_m = 175.8 μM) expressed as transport rate (nmol/mg protein/min) over LY concentration (μM) after 2.5 min incubation with LY at pH 5. Each data point represents the mean ± SE from triplicate determinations. Dotted lines represent confidence intervals.

3.2.2. Interaction screening

Due to the fact that mammalian OATP2B1 displays an increased transport activity, as well as an increase in substrate recognition at acidic pH, we decided to perform interaction experiments in acidic conditions (pH 5).

The initial screening revealed interactions with a wide range of physiological compounds, as well as xenobiotics, confirming polyspecific substrate specificity of zebrafish Oatp2b1 (Fig. 8). It showed major interactions with steroid and thyroid hormones and bilirubin. The most potent interaction was observed with bilirubin, which resulted in a complete inhibition of LY uptake upon co-exposure of Oatp2b1 transfected cells with 100 μM bilirubin. Triiodothyronine (T3), pregnenolone sulfate, T4, ethynyl-testosterone, progesterone and 17α-ethynylestradiol also strongly inhibited Oatp2b1 transport, resulting in only 1.8%, 4.6%, 7.2%, 11.7%, 12.6% and 17% LY uptake remaining in comparison with control (100%), respectively. From the group of xenobiotics, the strongest interaction was seen with bromosulfophthalein (BSP), perfluorooctanesulfonic acid (PFOS), diclofenac, perfluorooctanoic acid (PFOA), atorvastatin and tetracycline (0%, 1.8%, 2.5%, 7%, 14.5% and 15.1%, respectively).

3.2.3. Dose-response assays.

After the initial screening of the described series of compounds, the most potent interactors were selected for detailed dose-response analyses and determination of their IC_{50} values. Oatp2b1 showed the strongest interaction with cholic acid (IC_{50} = 0.7 µM), BSP (IC_{50} = 0.83 µM) and pregnenolone sulfate (IC_{50} = 4.99 µM). Further compounds that inhibited LY uptake over 80% were PFOS, diclofenac and sulfasalazine with IC_{50} values of 11.93, 13.16 and 15.75, respectively (Table 1; Fig. S2 and Fig. S3 in Supplementary Material).

Table 1
Overview of kinetic parameters and types of interaction determined for the strongest interactors of zebrafish Oatp2b1.

	IC_{50} (µM)	V_{max}	c.i.	K_m	c.i.	toi*
Control (LY)		**51.45**	45.69–57.2	**175,8**	128–223.5	
Bilirubin	**34.26**	**-**	-	-	-	-
Sulfasalazine	**15.75**	**-**	-	-	-	-
17α-Ethynylestradiol	**34.46**	**-**	-	-	-	-
Diclofenac	**13.16**	**23.8**	10.97–36.62	342.7	0.0-690.6	**I**
Ibuprofen	**49.45**	**-**	-	-	-	-
PFOA	**24.75**	**-**	-	-	-	-
PFOS	**11.93**	**32.14**	20.47–43.8	297.7	89.95–505.3	**I**
BSP	**0.83**	**45.09**	27.65–62.54	594.2	233.6-954.8	**S**
pregnenolone sulfate	**4.99**	**71.51**	42.07–101.0	877.7	369.3–1386	**S**
cholic acid	**0.7**	**-**	-	-	-	-

*toi – type of interaction

3.2.4. Determining the type of interaction.

After a determination of the IC_{50} values, the type of interaction for the strongest Oatp2b1 interactors was determined using Michaelis-Menten kinetics determinations (Table 1, Fig. S4 in Supplementary Material). BSP and pregnonolone sulfate were identified as substrates, while diclofenac and PFOS turned out to be inhibitors of Oatp2b1.

4. Discussion

The data shown in this study represent the first insights related to the structure, substrate preferences and possible function of zebrafish Oatp2b1. The transporter was first identified and classified in 2010 by Popovic et al. It showed a ubiquitously high expression with a tissue expression pattern similar to mouse

Oatp2b1. Membrane topology analysis revealed a high probability that zebrafish Oatps have 12 TMDs and that the organization of TMDs and LPs is highly conserved. Conserved motifs specific for Oatp superfamily were also identified in zebrafish Oatps: superfamily signature, a large extracellular loop 5 with ten conserved cysteines and Kazal SLC21 domain. Human OATP2B1 is a 709-amino acid and 85 kDa large glycoprotein containing 12 putative transmembrane-spanning domains (Hagenbuch, 2004; Grube et al., 2006). As revealed by western blot analysis, the zebrafish Oatp2b1 protein obtained in this study was about 85 kDa in size which corresponds to the size of human OATP2B1. However, as its predicted protein size based on nucleotide sequence is 75 kDa, we suggest that zebrafish Oatp2b1 is most probably glycosylated. N-glycosylation could be important for membrane localization, similarly as has been shown for another zebrafish Oatp, a teleost specific Oatp1d1 (Popovic et al., 2013). Our immunofluorescence analysis clearly demonstrated localization of Oatp2b1 inside the membrane of transiently transfected HEK293T cells, showing it is correctly localized and likely functionally active in the used expression system. Several other immunolocalization studies have also shown that OATP2B1 is primarily expressed in the plasma membrane (Kindla et al., 2011; Kleberg et al., 2012; Knauer et al., 2010; Le Vee et al., 2013).

Crystal structures are not yet available for any OATP/Oatp transporter. Yet, the comparison of *in silico* predicted protein structures of human OATP2b1 versus zebrafish Oatp2b1 obtained in this study (Figs. 3 and 4) clearly revealed significant similarities between the two transporters, which is further supported by a successful molecular docking of model substrate LY (Fig. 5). However, closer inspection reveals that in the case of zebrafish, LY is predicted to be placed slightly lower in the central pore. A possible explanation could be deduced from the above mentioned slightly narrower central pore in case of zebrafish Oat2b1, where a more constricted channel providing a more secured fit around the substrate molecule could be easily guiding LY through the channel in a more directed manner, leaving less space available for substrate rotation that could cause its lagging. Taken together, although constructed homology models cannot offer the same level of reliability and insights that can be obtained by protein crystallography, we believe that the models obtained in this study can be used for further molecular docking studies aimed at determining interactions of OATP2b1/Oatp2b1 with various physiological and xenobiotic substances.

After identifying the zebrafish Oatp2b1 protein and confirming its correct localization in HEK293T cell membranes, we verified LY as the model fluorescent substrate that could be used in transport activity assays and subsequent high-throughput screening protocols to obtain better insights into zebrafish Oatp2b1 interaction preferences. LY showed high accumulation into transfected cells and followed classical Michaelis-Menten kinetics. Considering that human OATP2B1 shows pH-dependent transport activity, where an increased transport activity was observed in acidic pH, we tested the transport of model substrate in both physiological (pH 7.4) and acidic conditions (pH 5). Similarly as was reported for human OATP2B1, we observed an increase of LY transport in acidic conditions (Fig. 7). The pH dependency of OATP2B1 is considered to be driven by the proton gradient, which likely plays a physiological role in the uptake of compounds from the intestinal lumen where pH is weakly acidic (Tamai, 2012). Furthermore, several mutagenesis studies have shown that pH dependency is probably

linked to a highly conserved histidine in the third transmembrane domain (Leuthold et al. 2009; Hagenbuch and Stieger, 2013).

Based on the expression profile and phylogenetic analysis which showed that zebrafish Oatp2b1 was phylogenetically closest to mammalian OATP2B1/Oatp2b1, Popovic et al. (2010) proposed that it is possibly a functional ortholog of OATP2B1. Based on this presumption, we tested some of the OATP2B1 interactors and similar anionic compounds for interaction with zebrafish Oatp2b1. As human OATP2B1 showed an increase in transport activity and number of substrates recognized at acidic pH, we performed the initial interaction screening at pH 5. Within potential physiological substrates, we observed the highest interaction with cholic acid, pregnenolone sulfate and bilirubin. Interaction with bile acids, steroid sulfates and thyroid hormones and bilirubin indicates a functional similarity with OATP2B1 (Al Sarakbi et al., 2006; Bronger et al., 2005; Köck et al., 2010). As the majority of the endogenous substrates of human OATP2B1 are steroid hormones and bile acids, its presumed physiological role is to assist in the distribution and elimination of regulatory compounds. Based on our results, the same could be the case for zebrafish Oatp2b1, although more studies and tests on a higher number of substances should be done to confirm this hypothesis.

On the other side, xenobiotics that showed the strongest interaction with zebrafish Oatp2b1 were BSP, PFOS, diclofenac and sulfasalazine, and BSP was identified as a substrate. BSP and sulfasalazine are also high-affinity substrates of human OATP2B1 with determined K_m value of 0.7 μM (Kullak-Ublick et al., 2001) and 1.7 μM (Kusuhara et al., 2012), respectively. In addition, we identified ibuprofen and PFOS as inhibitors of Oatp2b1. For human OATP2B1 no specific inhibitors have been identified yet, though aliskerin, celiprolol and premetrexed could be candidates, as they are selective substrates (McFeely et al., 2019).

In conclusion, based on the interaction data observed in this study, we suggest that zebrafish Oatp2b1 could indeed be a functional ortholog of human OATP2B1. Yet, there are still many knowledge gaps related to data on the expression, localization, regulation and function of Oatp2b1, especially in non-mammalian species, including fish. Moreover, it is important to point out that the focus of regulatory agencies worldwide has been mostly on the hepatic OATPs, in particular 1B1 and 1B3 (Mcfeely et al., 2019). As more studies are emerging, highlighting the importance of OATP transporters in the uptake and disposition of many endobiotics and xenobiotics, including drugs, it has become obvious that more research should be directed towards this type of transporters. The same is true for zebrafish Oatp2b1, as it is the second most expressed Oatp in zebrafish liver. In addition to its highly probable physiological role, Oatp2b1 could be an integral part of cellular defense and its inhibition by environmental contaminants might be of considerable ecotoxicological relevance. Therefore, this study could serve as a base for further (eco)toxicological research on Oatp2b1-mediated uptake of endo- and xenobiotics in zebrafish as an important vertebrate model species.

Declarations

Funding - This study was financed by the Croatian Science Foundation (Project No. IP-2019-04-1147) and partially supported under the STIM-REI project, Contract Number: KK.01.1.1.01.0003, a project funded by the European Union through the European Regional Development Fund – Operational Programme Competitiveness and Cohesion 2014–2020 (KK.01.1.1.01).

Author contributions - JD designed and performed majority of cloning, transfection and interaction experiments, and wrote the manuscript; NM performed homology modelling and molecular docking studies; MP did initial cloning of zebrafish Oatp2b1; TS supervised the project, study conception and design, and wrote the manuscript with input from all authors. All of the authors reviewed the results and approved the final version of the manuscript.

Data availability – The datasets generated during and/or analysed during the current study are available from the corresponding author on reasonable request.

Conflict of Interest - The authors declare no competing interests.

References

Al Sarakbi W, Mokbel R, Salhab M, Jiang WG, Reed MJ, Mokbel K (2006) The role of STS and OATP-B mRNA expression in predicting the clinical outcome in human breast cancer. Anticancer Res 26:4985-4990.

Bronger H, König J, Kopplow K, Steiner HH, Ahmadi R, Herold-Mende C (2005) ABCC drug efflux pumps and organic anion uptake transporters in human gliomas and the blood-tumor barrier. Cancer Res 65:11419-11428.

Grube M, Köck K, Oswald S, Draber K, Meissner K, Eckel L, Böhm M, Felix SB, Vogelgesang S, Jedlitschky G, Siegmund W, Warzok R, Kroemer HK (2006) Organic anion transporting polypeptide 2B1 is a high-affinity transporter for atorvastatin and is expressed in the human heart. Clin Pharmacol Ther 80:607-20.

Hagenbuch B, Gui C (2008) Xenobiotic transporters of the human organic anion transporting polypeptides (OATP) family. Xenobiotica 38:778–801.

Hagenbuch B, Meier PJ (2003) The superfamily of organic anion transporting polypeptides. BBA Biomem 1609:1–18.

Hagenbuch B, Meier PJ (2004) Organic anion transporting polypeptides of the OATP/ SLC21 family: phylogenetic classification as OATP/SLCO superfamily, new nomenclature and molecular/functional properties. Pflugers Arch 447:653–665.

Hagenbuch B, Stieger B (2013) Molecular Aspects of Medicine The SLCO (former SLC21) superfamily of transporters. Mol Aspects Med 34:396–412.

Kindla J, Fromm MF, König J (2009) *In vitro* evidence for the role of OATP and OCT uptake transporters in drug–drug interactions. Exp Opin Drug Metab Toxicol 5:489–500.

Kindla J, Rau TT, Jung R, Fasching PA, Strick R, Stoehr R (2011) Expression and localization of the uptake transporters OATP2B1, OATP3A1 and OATP5A1 in non-malignant and malignant breast tissue. Cancer Biol Ther 11:584–91.

Kleberg K, Jensen GM, Christensen DP, Lundh M, Grunnet LG, Knuhtsen S, Poulsen SS, Berner Hansen M, Bindslev N (2012) Transporter function and AMP turnover in normal colonic mucosa from patients with and without colorectal neoplasia. BMC Gastroenter 12:78.

Köck K, Koenen A, Giese B, Fraunholz M, May K, Siegmund W, Hammer E, Völker U, Jedlitschky G, Kroemer HK, Grube M (2010) Rapid modulation of the organic anion transporting polypeptide 2B1 (OATP2B1, SLCO2B1) function by protein kinase C-mediated internalization. J Biol Chem 285:11336–11347.

Kullak-Ublick GA, Ismair MG, Stieger B, Landmann L, Huber R, . Pizzagalli F, Fattinger K, Meier PJ, Hagenbuch B (2001) Organic anion-transporting polypeptide B (OATP-B) and its functional comparison with three other OATPs of human liver. Gastroenter 120:525-533.

Kusuhara H, Furuie H, Inano A, Sunagawa A, Yamada S, Wu C, Fukizawa S, Morimoto N, Ieiri I, Morishita M, Sumita K, Mayahara H, Fujita T, Maeda K, Sugiyama Y (2012) Pharmacokinetic interaction study of sulphasalazine in healthy subjects and the impact of curcumin as an in vivo inhibitor of BCRP. Br J Pharmacol 166:1793-803.

Le Vee M, Noel G, Jouan E, Stieger B, Fardel O (2013) Polarized expression of drug transporters in differentiated human hepatoma HepaRG cells. Toxicol in Vitro 27:1979–1986.

Leuthold S, Hagenbuch B, Mohebbi N, Wagner CA, Meier PJ, Stieger B (2009) Mechanisms of pH-gradient driven transport mediated by organic anion polypeptide transporters. Am J Physiol Cell Physiol 296: C570–582.

McFeely SJ, Wu L, Ritchie TK, Unadkat J (2019) Organic Anion Transporting Polypeptide 2B1 – More than aGlass-Full of Drug Interactions. Pharmacol Ther 196:204-215.

Meier-Abt F, Mokrab Y, Mizuguchi K (2005) Organic anion transporting polypeptides of the OATP/SLCO superfamily: identification of new members in nonmammalian species, comparative modeling and a potential transport mode. J Membr Biol 208:213–227.

Nozawa T, Imai K, Nezu JI, Tsuji A, Tamai I (2004) Functional characterization of pH sensitive organic anion transporting polypeptide OATP-B in human. J Pharmacol Exp Ther 308: 438–445.

Popovic M (2014) Identification, characterization and ecotoxicological relevance of membrane transport protein families Slc21 and Slc22 in zebrafish (Danio rerio Hamilton, 1822). PhD thesis. Josip Juraj Strossmayer University of Osijek.

Popovic M, Zaja R, Fent K, Smital T (2013) Molecular characterization of zebrafish Oatp1d1 (Slco1d1), a novel Organic anion transporting polypeptide. J Biol Chem 288:33894-33911.

Popovic M, Zaja R, Smital T (2010) Organic anion transporting polypeptides (OATP) in zebrafish (*Danio rerio*): phylogenetic analysis and tissue distribution. Comp Biochem Physiol A 155:327-335.

Roth M, Obaidat A, Hagenbuch B (2012). OATPs, OATs and OCTs: the organic anion and cation transporters of the SLCO and SLC22A gene superfamilies. Br J Pharmacol 165:1260–1287.

Sai Y, Kaneko Y, Ito S, Mitsuoka K, Kato Y, Tamai I, Artursson P, Tsuji A (2006) Predominant contribution of organic anion transporting polypeptide OATP-B (OATP2B1) to apical uptake of estrone-3-sulfate by human intestinal Caco-2 cells. Drug Metab Disp 34:1423–1431.

Tamai I, Nezu J, Uchino H, Sai Y, Oku A, Shimane M, Tsuji A (2000) Molecular identification and characterization of novel members of the human organic anion transporter (OATP) family. Biochem Biophys Res Commun 273:251–260.

Tamai I (2012) Oral drug delivery utilizing intestinal OATP transporters. Adv Drug Deliv Rev 64:508–514.

Figures

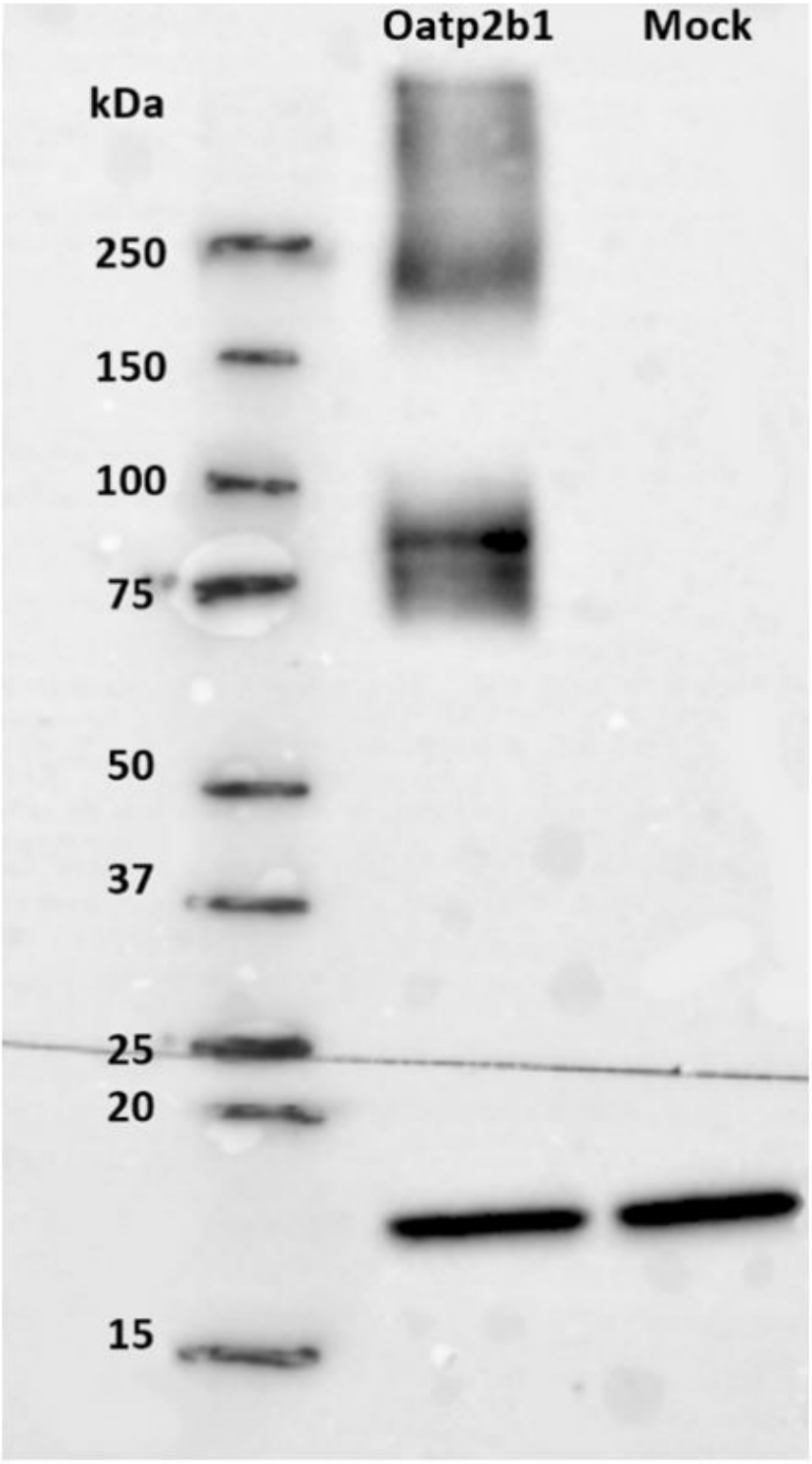

Figure 1

Western blot analysis of zebrafish Oatp2b1 transporter expressed in transfected versus mock transfected cells. Total cell lysate revealed protein band of Oatp2b1 that corresponds to the size of glycosylated monomeric protein, or possible homo- or heterodimeric forms and post-translational modifications.

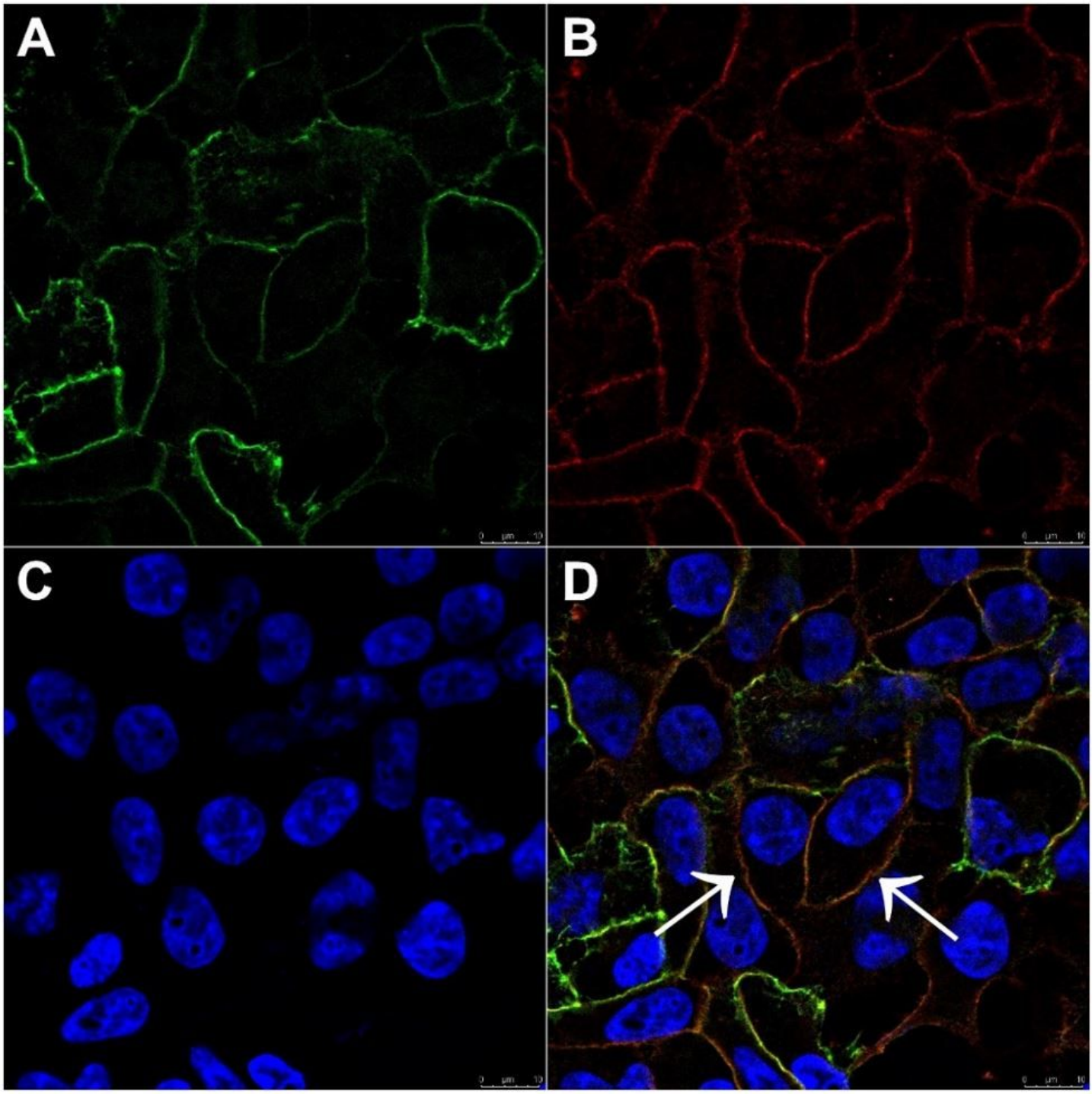

Figure 2

Immunolocalization of zebrafish Oatp2b1 by co-localization of the green colored Oatp2b1 and the red colored Na/K ATPase. The signals of the two dyes were combined, resulting in an orange signal which confirmed the localization within the cell membrane. Nuclei are stained with DAPI (blue).

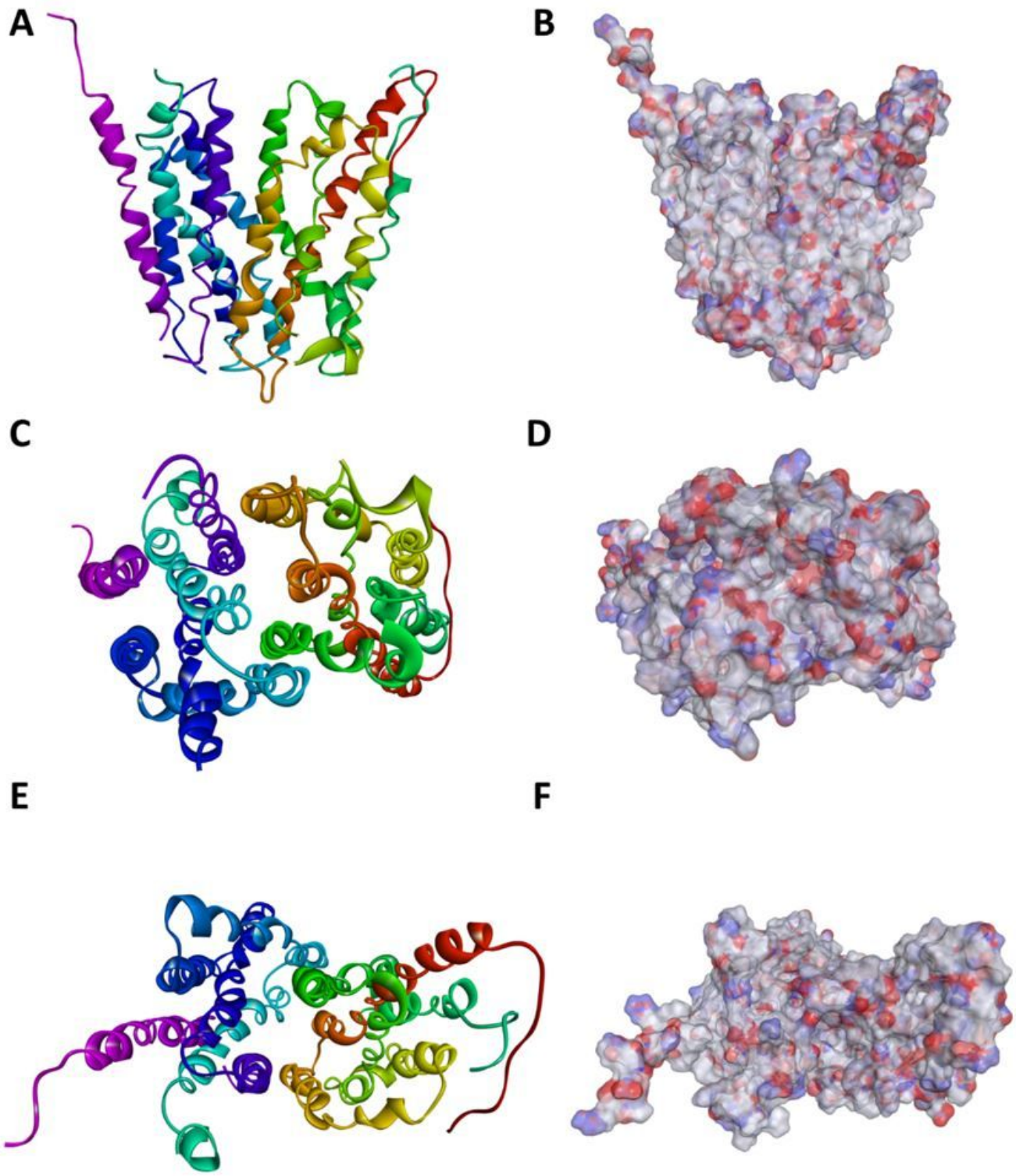

Figure 3

Solid ribbon and rainbow-colored representation of the homology model of human OATP2b1 as viewed from the lateral side (A), the extracellular side (C) and the intracellular side (E) with electrostatic potential mapped onto its molecular surface, respectively (B, D, F). Regions of negative, positive and neutral potential are shown in red, blue and white/gray, respectively.

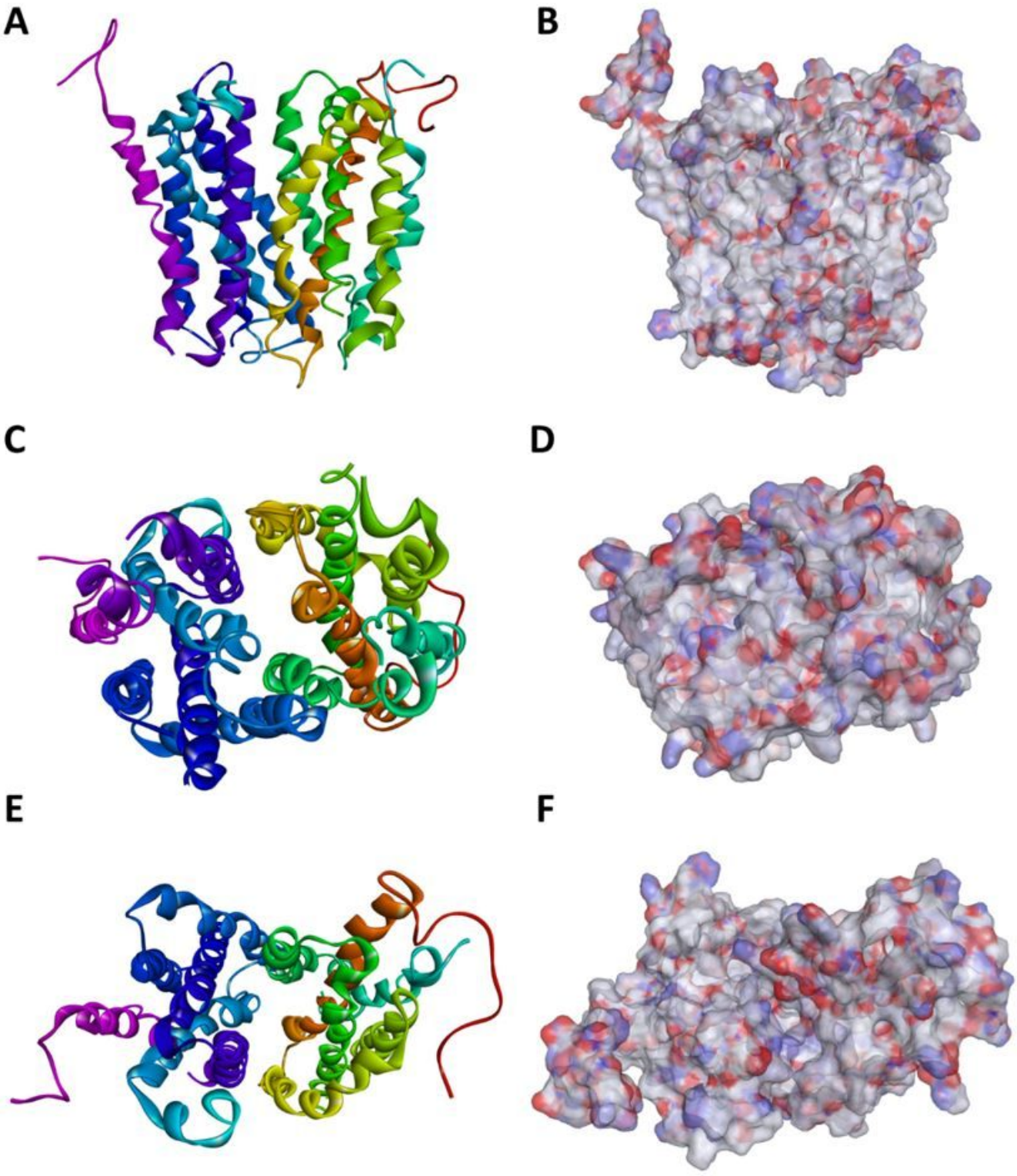

Figure 4

Solid ribbon and rainbow-colored representation of the homology model of zebrafish Oatp2b1 as viewed from the lateral side (A), the extracellular side (C) and the intracellular side (E) with electrostatic potential mapped onto its molecular surface, respectively (B, D, F). Regions of negative, positive and neutral potential are shown in red, blue and white/gray, respectively.

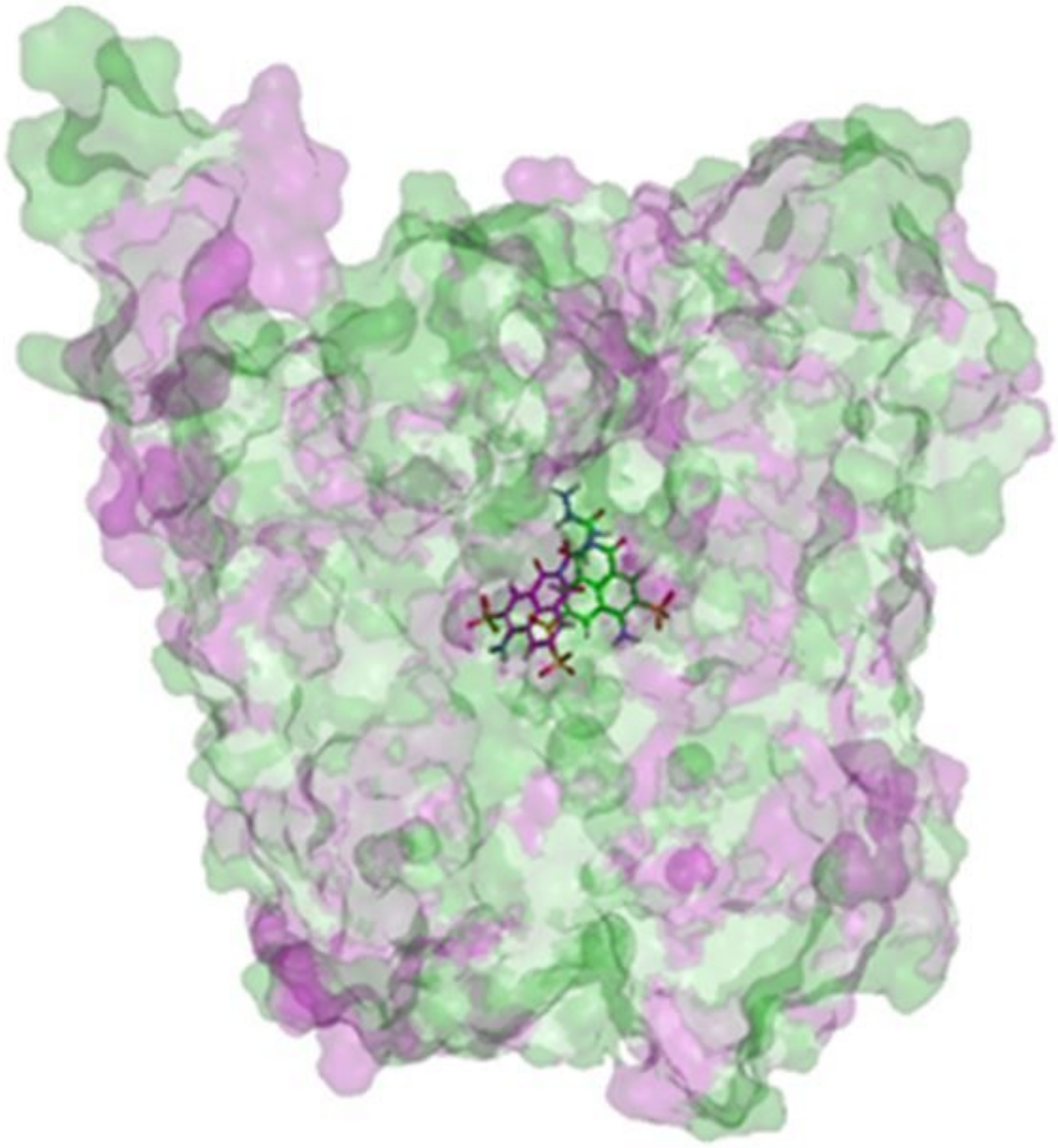

Figure 5

Superposition of model complexes between human OATP2b1 (carbon atoms in green) or zebrafish Oatp2b1 (carbon atoms in magenta) and LY, respectively.

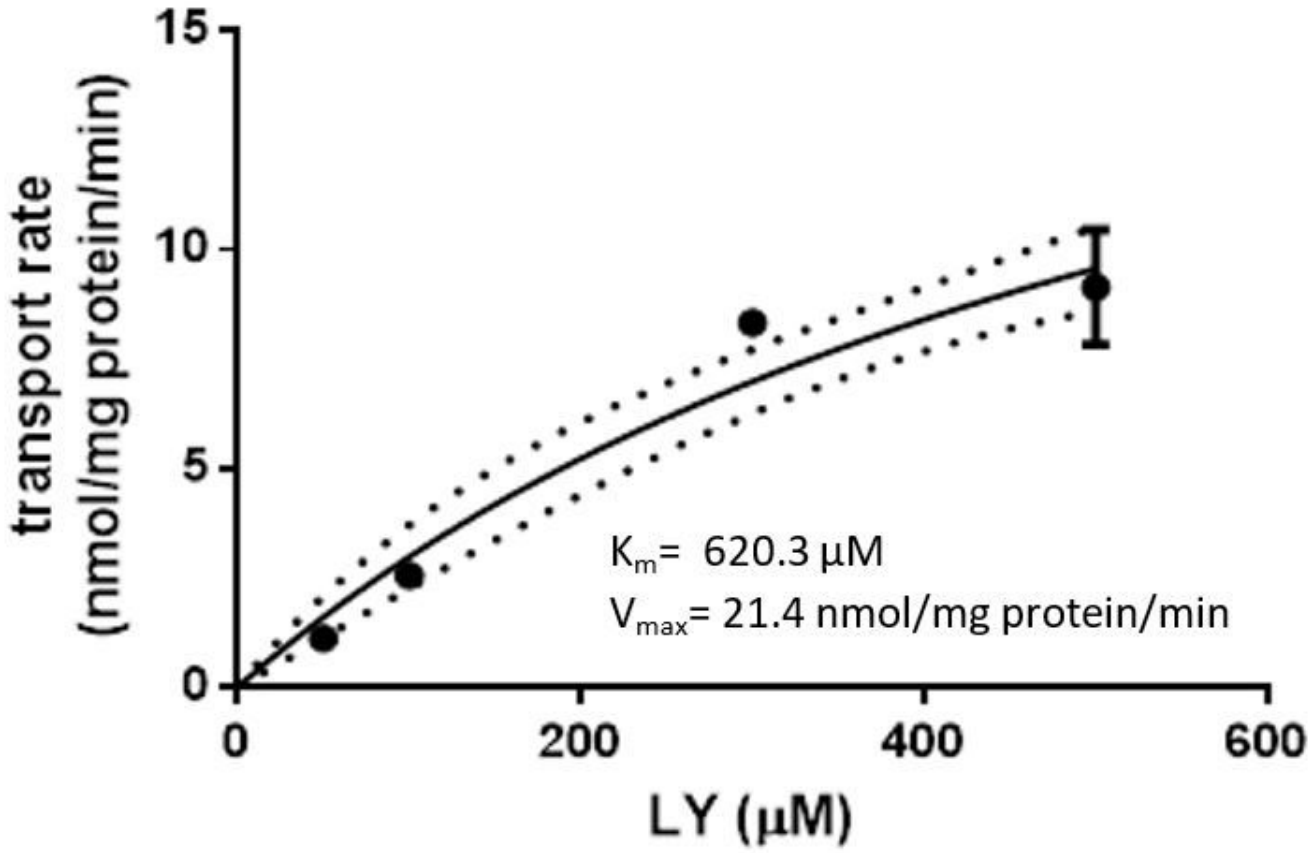

Figure 6

Dose-response of zebrafish Oatp2b1 transport of the fluorescent model substrate LY (Km = 620.3 µM) expressed as transport rate (nmol/mg protein/min) over LY concentration (µM) after 2.5 min incubation with LY at pH 7.4. Each data point represents the mean ± SE from triplicate determinations. Dotted lines represent confidence intervals.

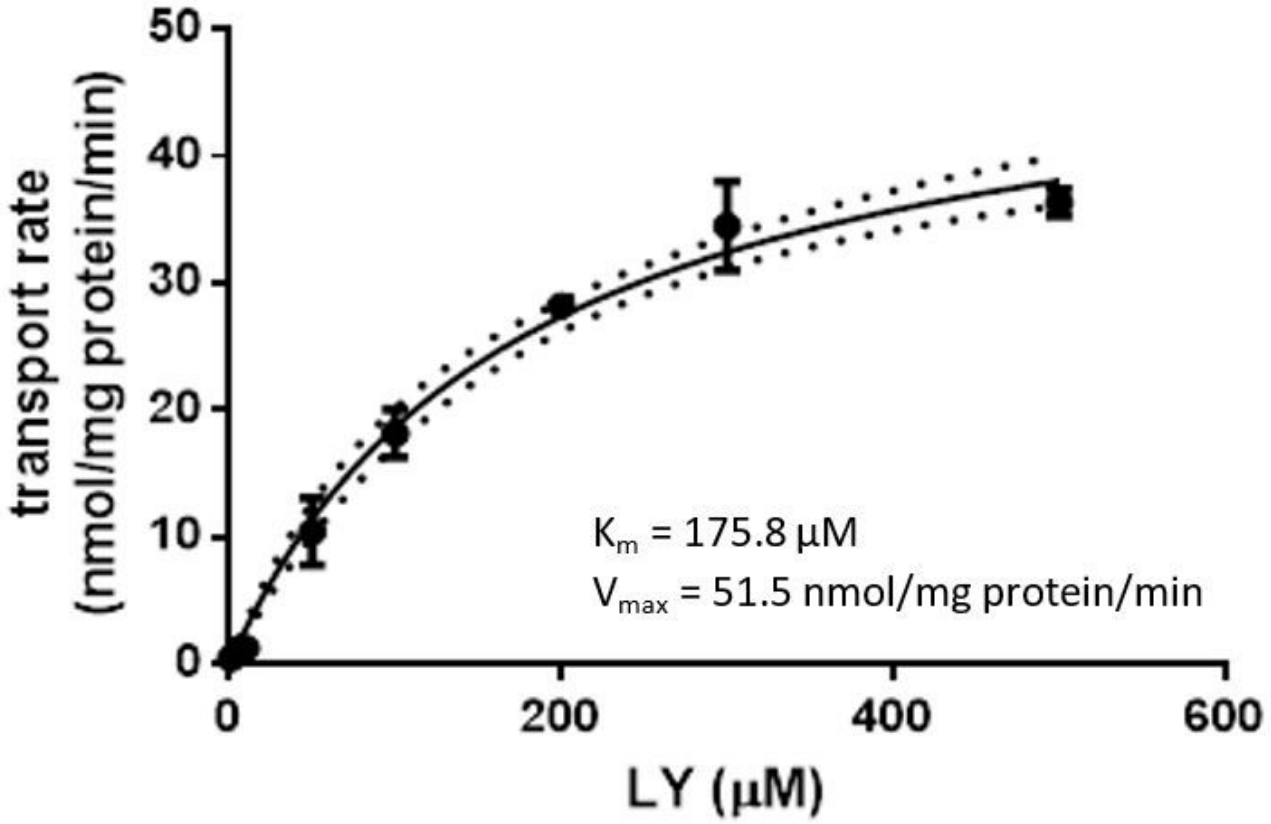

Figure 7

Dose-response of zebrafish Oatp2b1 transport of the fluorescent model substrate LY (Km = 175.8 µM) expressed as transport rate (nmol/mg protein/min) over LY concentration (µM) after 2.5 min incubation with LY at pH 5. Each data point represents the mean ± SE from triplicate determinations. Dotted lines represent confidence intervals.

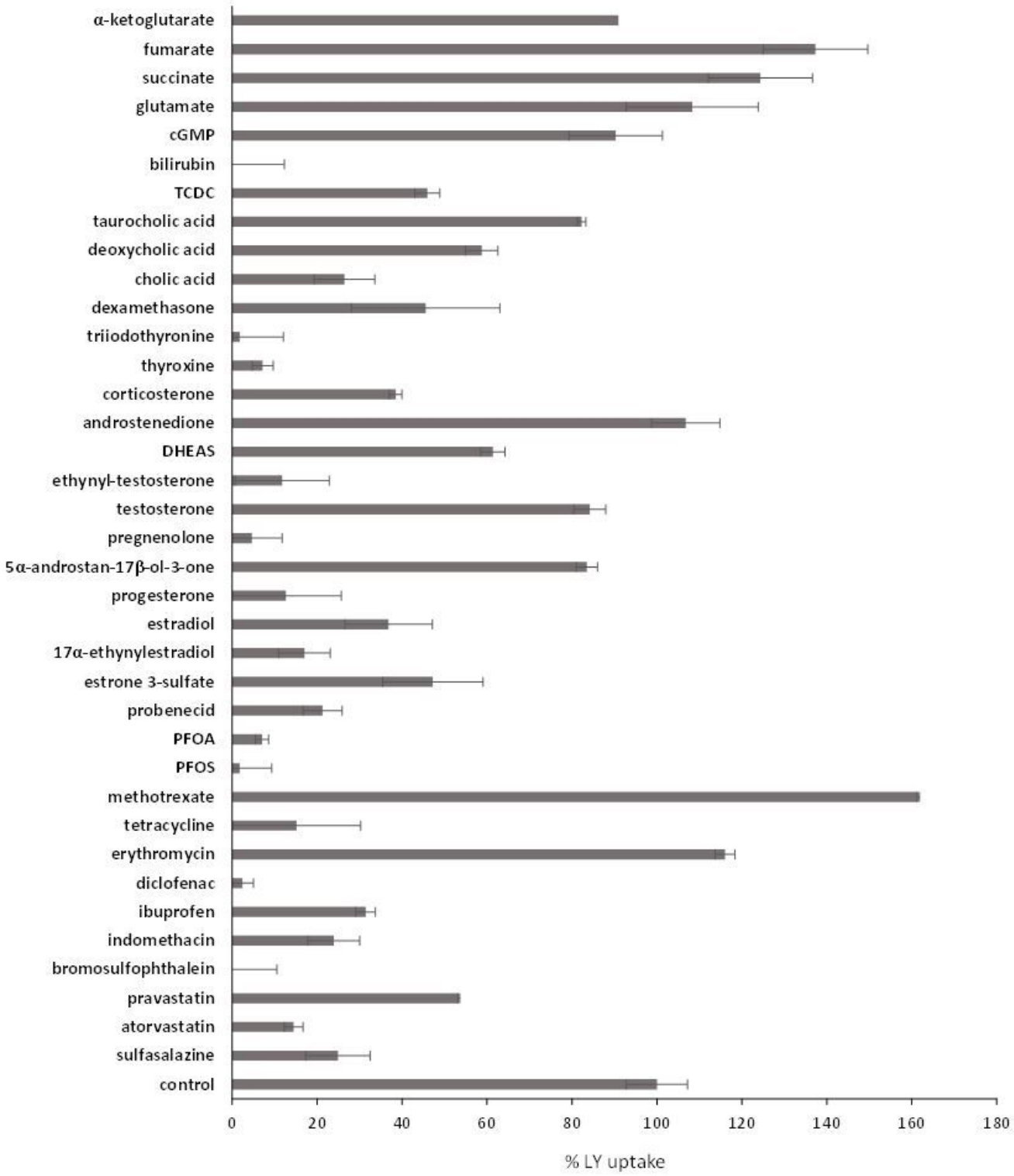

Figure 8

Interaction of zebrafish Oatp2b1 with known interactors of mammalian Oatp subfamily members and similar anionic compounds. Data are expressed as mean percentage (%) ± SD from triplicate determinations of LY uptake after co-incubation with each interactor (100 μM) relative to LY uptake in the absence of an interactor which is set to 100% (control).